Pulsed Optical Parametric Generation, Amplification, and Oscillation in Monolithic Periodically Poled Lithium Niobate Crystals

An-Chung Chiang, Tsong-Dong Wang, Yen-Yin Lin, Chee-Wai Lau, Yen-Hung Chen, Bi-Cheng Wong, Yen-Chieh Huang, *Member, IEEE*, Jow-Tsong Shy, Yu-Pin Lan, Yung-Fu Chen, and Pei-Hsi Tsao

***Abstract*—We conducted a series of passively Q-switched Nd:YAG laser pumped optical parametric generation, amplification, and oscillation experiments in monolithic periodically poled lithium niobate (PPLN) crystals. Double-pass optical parametric generation with an effective gain length of 10 cm in a PPLN crystal was performed in comparison with single-pass operation in the same crystal. By seeding a PPLN optical parametric amplifier with a distributed feedback (DFB) diode laser, we produced 200-ps transform-limited laser pulses at 1549.6 nm and observed parametric gain competition at different pump levels. For optical parametric oscillations, we first demonstrated 22% power efficiency from a 2.4-cm intrinsic-cavity PPLN optical parametric oscillator pumped by a 4.2-ns, 10-kW passively Q-switched Nd:YAG laser. Preliminary studies on DFB optical parametric oscillators in PPLN are mentioned. The temporal and spectral properties of these optical parametric generators, amplifiers, and oscillators are characterized and discussed.**

***Index Terms*—Nonlinear optics, optical parametric amplification, optical parametric generation, optical parametric oscillation, periodically poled lithium niobate (PPLN), quasi-phase-matching (QPM).**

I. Introduction

THE optical parametric process has been an attractive means for generating wavelength tunable laser radiation since the establishment of its theory in the 1960s and 1970s [1]–[3]. Due to its wide wavelength tuning range, laser sources based on the optical parametric technique have been used in numerous applications. Quasi-phase-matching (QPM) nonlinear frequency conversion [4] has the advantages of having no Poynting vector walkoff, permitting the selection of the largest nonlinear coefficient, and designing the mixing wavelengths through lithographic patterning techniques [5], [6]. Among all of the QPM crystals, periodically poled lithium niobate (PPLN) [7] is particularly attractive due to its available large crystal size, broad transparent range, large nonlinear coefficient, and low cost. However, several adverse effects associated with a PPLN crystal were also discovered during the development of PPLN-based laser sources. For example, photorefractive damage [8], thermal lensing, and green-induced infrared absorption [9] are the three major issues hindering congruent PPLN crystals from being used in the visible spectrum. Despite the effort in doping lithium niobate with Mg or Zn ions to alleviate these effects [10], reliable, large-size, and economic impurity-doped PPLN crystals for visible laser applications are not yet available. In the infrared spectrum, the aforementioned adverse effects are less obvious although not completely vanished. Consequently, PPLN-based mid-infrared lasers have been considered as useful and practical sources for a number of applications [11]–[13].

Due to the high coercive field of congruent lithium niobate, congruent PPLN crystals are mostly available with a thickness less than 1 mm. The performance of a PPLN-based infrared laser is therefore more restricted to laser-intensity damage and power handling capability in such a thin laser aperture. Different pump lasers for PPLN-based frequency converters have different limitations. For example, an actively Q-switched pump laser is likely to cause laser-intensity damage, a mode-locked pump laser is complex and has the problem of group velocity walk-off, and a CW pumped optical parametric oscillator requires a high-average power to achieve the oscillation threshold. In addition, an optical parametric oscillator often requires external resonator mirrors, which adds complexity and cost to a laser system.

In this paper, we employed Nd:YAG microchip lasers passively Q-switched (PQS) by Cr:YAG saturable absorbers as the pump sources for optical parametric generation (OPG), amplification (OPA) and oscillation (OPO) in PPLN crystals. The first section of this paper describes the theory and experiment of pump-depleted OPG. The second section describes OPO in monolithic PPLN crystals. A passively Q-switched Nd:YAG microchip laser has the advantages of compactness, low cost, single-frequency output, and moderate peak power. Since laser damage fluence is proportional to the square root of a laser pulse width in the thermal-damage-limited regime [14], a PQS laser, having a typical pulse width one tenth that of an actively Q-switched laser, is less likely to damage a PPLN crystal and yet produces enough peak power for efficient nonlinear-frequency conversions. To further enhance the conversion efficiency, we demonstrated a double-pass PPLN OPG

Manuscript received September 19, 2003; revised February 26, 2004. This work was supported by the National Science Council of Taiwan under Contract NSC92-2622-L007-002 and by HC Photonics Company, Taiwan, under National Tsinghua University Project 90A0123J6.

A.-C. Chiang, T.-D. Wang, Y.-Y. Lin, C.-W. Lau, Y.-H. Chen, B.-C. Wong, and Y.-C. Huang are with the Department of Electrical Engineering, National Tsinghua University, Hsinchu 300, Taiwan (e-mail: acchiang@ee.nthu.edu.tw; ychuang@ee.nthu.edu.tw).

J.-T. Shy is with the Department of Physics, National Tsinghua University, Hsinchu 300, Taiwan.

Y.-P. Lan and Y.-F. Chen are with the Department of Electrophysics, National Chiaotung University, Hsinchu 300, Taiwan.

P.-H. Tsao is with the Department of Physics, National Taiwan University, Taipei 106, Taiwan.

Digital Object Identifier 10.1109/JQE.2004.828269

0018-9197/04$20.00 © 2004 IEEE

laser and characterized the temporal and spectral properties of such a laser against a single-pass one. By using a PQS Nd:YAG pump laser and a narrow-line seeding diode laser, we further accomplished a pulsed PPLN OPA laser with a transform-limited output linewidth. For PPLN OPO, we accomplished and characterized an ultracompact, planar-mirror-resonator optical parametric oscillator in a 2.4-cm-long monolithic PPLN crystal with dielectric-mirror coatings to the end faces of the crystal. We conclude the OPO section by mentioning some studies on distributed feedback (DFB) optical parametric oscillators in monolithic PPLN crystals.

II. Optical Parametric Generation and Amplification

A. Theory of Pump-Depleted Optical Parametric Generation

OPG produces laser-like radiation with an energy level comparable to the pump in one pump transit. The optical output results from the amplification of an input noise photon in either the signal or idler channel. In this section, we first present a theory for pump-depleted OPG. We then compare the experimental performance of single-pass and double-pass optical parametric generators against the theory.

Throughout this paper, we define the coordinates consistent with the PPLN crystallographic coordinate system for nonlinear frequency mixing. Specifically, the mixing waves propagate in the x direction and are all polarized in the z direction. For a noise photon in the signal channel, the single-pass intensity gain for OPG without pump depletion in a lossless nonlinear optical material is given by [15]

$$G(L) = \frac{I_s(L)}{I_s(0)} = \Gamma^2 L^2 \frac{\sinh^2 gL}{(gL)^2} \tag{1}$$

where $I_s(0)$ is the initial optical intensity of a signal photon, $I_s(L)$ is the signal intensity after a gain distance L, $\Gamma = [2\omega_s\omega_i d_{eff}^2 I_p/\varepsilon_0 c^3 n_s n_i n_p]^{1/2}$ is the phase-matched gain coefficient, $g = \sqrt{\Gamma^2 - (\Delta k/2)^2}$ is the overall gain coefficient including phase mismatch $\Delta k = k_p - (k_s + k_i)$, ω is the angular frequency of the wave, n is the refractive index, c is the vacuum wave velocity, ε_0 is the vacuum permittivity, d_{eff} is the effective nonlinear coefficient of the material, and I_p is the undepleted pump intensity. In obtaining (1), collinear plane waves with slowly varying envelopes are assumed in the nonlinear optical material. It is clearly seen from (1) that the signal power grows exponentially in the high-gain regime given by $G(L) \propto \exp(2\Gamma L)$ for $\Gamma \gg \Delta k$.

From (1), we calculate the full-width at half-maximum (FWHM) value of the low-gain ($\Gamma \ll \Delta k$) and high-gain ($\Gamma \gg \Delta k$) bandwidths to be $\Delta k_{low-gain} = 0.886\pi/L$ and $\Delta k_{high-gain} = (4\Gamma \ln 2/L)^{1/2}$, respectively. The high-gain bandwidth increases with the parametric gain as more noise photons of different wavelengths are able to acquire enough parametric gain and grow to a significant energy level. The ratio of the high-gain to low-gain FWHM bandwidths is therefore given by

$$\frac{\Delta k_{\mathrm{high-gain}}}{\Delta k_{\mathrm{low-gain}}} \cong 0.6\sqrt{\Gamma L}. \tag{2}$$

Pump depletion usually occurs in an OPG process when the generated signal energy is comparable to the pump one. To calculate pump depletion, one usually has to go through fairly complex procedures and solve the three coupled-wave differential equations simultaneously [1]. A simplified model for pump-depleted OPG can be obtained by assuming a pump-intensity-dependent exponential gain throughout the crystal length. The assumption is valid in the strong exponential-gain regime, because this model is equivalent to dividing the nonlinear crystal into several cascaded OPG sections with each section having exponential gain and an initial pump intensity equal to the depleted pump intensity from the previous section. According to this model, the specific form of the gain expression is given by

$$G = \frac{I_s(L)}{I_s(0)} \approx \exp\left[2\int_0^L \Gamma(x)\cdot dx\right] \tag{3a}$$

or

$$\frac{dI_s(x)}{dx} \approx 2\Gamma(x) I_s(x) \tag{3b}$$

where $\Gamma(x) = [2\omega_s\omega_i d_{eff}^2 I_p(x)/\varepsilon_0 c^3 n_s n_i n_p]^{1/2}$ is the pump-intensity-dependent gain coefficient. For OPG starting from a vacuum noise, $I_s(0) \ll I_p(0)$ and $I_i(0) \ll I_p(0)$, and the expression

$$I_p(x) \approx I_p(0) - [I_s(x) + I_i(x)] = I_p(0) - I_s(x) \times \frac{\omega_p}{\omega_s} \tag{4}$$

is valid under the energy conservation and the Manley–Rowe relation. Substituting (4) into (3b) and solving for $I_s(L)$, the signal output intensity in the pump-depleted OPG process becomes

$$I_s(L) = \frac{\omega_s}{\omega_p} I_p(0)\left[\left(\frac{1+A}{1-A}\right)^2 - 1\right] \tag{5}$$

where

$$\begin{aligned} A &\equiv \left|\frac{\sqrt{I_p(0) + I_s(0)\omega_p/\omega_s} - \sqrt{I_p(0)}}{\sqrt{I_p(0) + I_s(0)\omega_p/\omega_s} + \sqrt{I_p(0)}}\right| \exp[2\Gamma(0)L] \\ &\approx \frac{I_s(0)/\omega_s)}{4I_p(0)/\omega_p} \exp[2\Gamma(0)L]. \end{aligned}$$

Equation (5) is reduced to the undepleted-pump gain expression for $A \ll 1$.

B. Optical Parametric Generation

Zayhowski first showed the great potential of a PQS-laser pumped PPLN optical parametric generator [16] and measured the temporal behavior of such a source. In this paper, we further extend this potential to several uniquely designed PQS-laser-pumped optical parametric devices in monolithic PPLN crystals and characterize their spectral performance.

First, we fabricated a 0.5-mm-thick, 5-cm-long PPLN crystal comprising seven PPLN gratings with the grating vectors aligned parallel to the pump laser beam. The periods of the PPLN gratings varied from 28 to 31 μm in 0.5-μm increments. The pump laser used in this experiment was an Nd:YAG microchip laser passively Q-switched by a Cr:YAG saturable absorber, producing 9-μJ pulse energy with 530-ps FWHM pulse width repeating at a 3.83-kHz rate. The PPLN end surfaces were optically polished without any optical coating. The round-trip time of an optical wave in the 5-cm-long PPLN

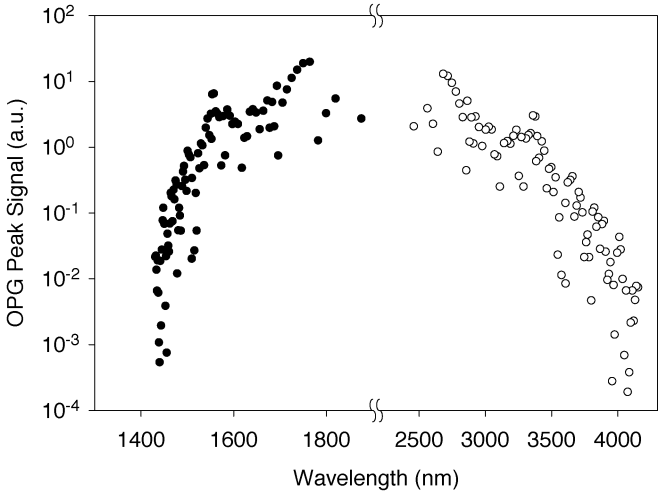

Fig. 1. Power spectrum of the 1064-nm pumped PPLN optical parametric generator for a constant pump intensity of 0.15 GW/cm^2. The multigrating PPLN crystal has periods varying from 28 to 31 μm in 0.5-μm increments. The solid dots are the peak signal intensities measured by an InGaAs detector with corrections from the detector's spectral response. The open dots are the corresponding idler intensities calculated from the Manley–Rowe relation.

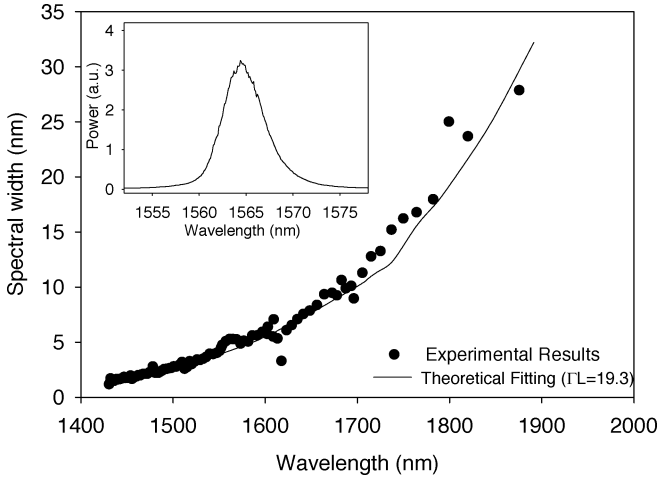

Fig. 2. Signal spectral width versus signal wavelength of the 1064-nm pumped optical parametric generator in the mutigrating PPLN crystal for a pump intensity of 0.15 GW/cm^2 ($\Gamma L \sim 19.3$). The continuous curve is the theoretical fitting curve calculated from (1) in conjunction with the Sellmeier equation of congruent lithium niobate. Inset: a typical signal spectrum centered at 1564.7 nm from the 30-μm period PPLN phase-matched at 75 °C.

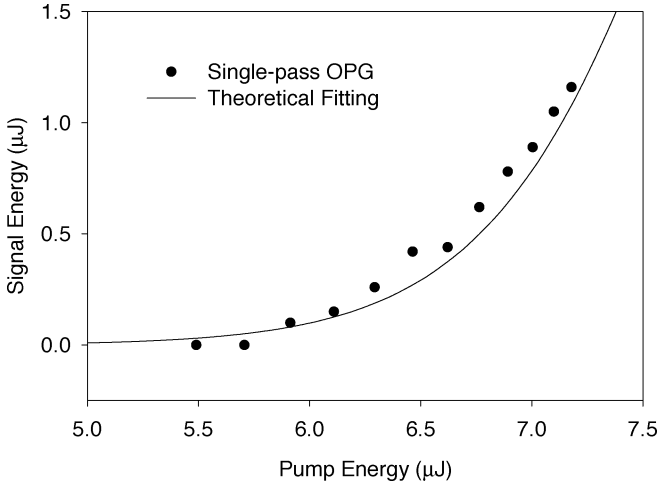

Fig. 3. Measured signal output energy versus pump energy from the 30-μm-period PPLN crystal phase-matched at 75 °C. The continuous curve is the theoretical prediction calculated from (5).

crystal is approximately 700 ps, which is longer than the pump pulse width. Therefore, in our experiment, the Fresnel reflections of the signal wave from the PPLN end faces did not contribute to the signal buildup in the PPLN crystal. We focused the laser beam to a 75-μm-radius ($1/e^2$-intensity) spot in the PPLN crystal. By varying the temperature from 35 °C to 165 °C in the multigrating PPLN crystal, we tuned the signal (idler) wavelength from 1430 (4157) to 1875 (2459) nm. The measured wavelength tuning range is consistent with the published Sellmeier equation [17]. Fig. 1 shows the power spectrum of the 1064-nm PQS-laser pumped PPLN optical parametric generator for a constant pump intensity of 0.15 GW/cm^2. The data in Fig. 1 were obtained by sampling the signal pulses in time and are equivalent to the single-shot measurement. Because the OPG process relies on parametric gain exceeding 10^{12}, the intensity fluctuations in the OPG outputs can be clearly seen from the single-shot power spectrum. Nonetheless, it is evident from this qualitative plot that the signal and idler power reduction on the two wings of the figure are due to the frequency dependence of $\Gamma \propto \sqrt{\omega_s \omega_i}$ off the degeneracy and slight idler absorption in lithium niobate and that at the center of the plot is due to phase mismatch in the 28–31-μm PPLN. Owing to the OH absorption near the 2.9-μm wavelength in lithium niobate, the power reduction at the 2.9-μm as well as at the 1.67-μm signal wavelength can also be seen in Fig. 1. Because a parametric process is a cooperative process, the absorption at the idler wavelength also suppresses the growth of the signal [18], [19].

Fig. 2 shows the averaged signal spectral width versus signal wavelength of the 1064-nm PQS-laser pumped optical parametric generator in the multigrating PPLN crystal with a pump intensity of 0.15 GW/cm^2 ($\Gamma L = 19.3$). The continuous line is the theoretical fitting curve from (1) in conjunction with the Sellmeier equation of congruent lithium niobate. The OPG bandwidth becomes broader when the signal and idler wavelengths approach the degeneracy wavelength of 2128 nm. The experimental result agrees reasonably well with the theoretical fitting curve. The inset of Fig. 2 is a typical signal spectrum centered at 1564.7 nm from the 30-μm period PPLN phase-matched at 75 °C. According to (2), the theoretical ratio of the high-gain-to-low-gain bandwidths is 2.4. Given the calculated 1.6-nm low-gain bandwidth, we obtained a bandwidth ratio of 2.8 from the inset for $\Gamma L = 19.3$. The slight deviation between the theoretical prediction and experimental result is attributable to the intrinsic OPG signal fluctuations in the high-gain regime. Fig. 3 shows the measured signal output energy versus pump energy from the 30-μm-period PPLN phase-matched at 75 °C. We achieved 14.9% signal conversion efficiency and 38.4% slope efficiency at the maximum pump energy of 7.4 μJ from our laser. For comparison, the theoretical fitting curve is shown in the same figure by plotting (5) with the assumptions of perfect phase matching $\Delta k = 0$ and one signal noise photon at the input.

Due to the exponential gain, the output pulse width from OPG can be much shorter than the pump pulse width [20].

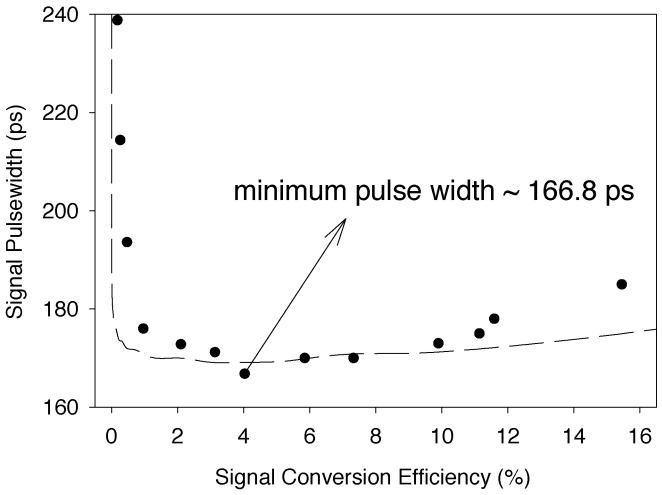

Fig. 4. Measured OPG signal pulse width versus pump-to-signal conversion efficiency from the 30-μm-period PPLN at 75 °C. The minimum pulse width (166.8 ps) occurred at 4% efficiency.

With pump depletion, the signal pulse width can be estimated by introducing time-dependent pump intensity in the simplified model as given by (5). Fig. 4 shows the measured OPG signal pulse width versus pump-to-signal conversion efficiency from the 30-μm-period PPLN OPG phase matched at 75 °C. The dashed line is the theoretical fitting curve calculated from (5). It is seen from the plot that the signal pulse width is quickly reduced from the pump one due to the strong nonlinear gain before strong pump depletion, but increases gradually due to pump depletion at high conversion. At 4% pump-to-signal conversion, we measured a minimum pulse width of 166.8 ps, as indicated in the plot. Since (5) is only valid in the exponential-gain or strong-pump regime throughout the entire crystal, the dashed line in Fig. 4 starts to deviate from the experimental data in the deeply pump-depleted limit. The simultaneous pulse compression and wavelength conversion in a controlled OPG process could be useful in certain applications.

C. Double-Pass Optical Parametric Generation

To increase the conversion efficiency of nonlinear wave mixing, a straightforward method is to increase the length of a nonlinear optical material. For a finite crystal size, the multipass scheme is an economic possibility for efficiency enhancement. Unlike other nonlinear frequency conversions requiring delicate phase corrections between crystal discontinuities [21], [22], multipass OPG automatically builds up from the phase-matched components in the broad gain bandwidth. Previously, Jeys *et al.* demonstrated an eight-pass optical parametric amplifier by using external elements including a prism, an achromatic lens, and a mirror [23]. We describe in the following a simple low-loss multipass optical parametric generator in a monolithic PPLN crystal. Fig. 5 shows the cutting configuration of the multipass PPLN crystal, wherein all the crystal surfaces (except surface 6) were optically polished. The 50 mm (length in x) × 7 mm (width in y) × (thickness in z) PPLN crystal has a QPM grating period of 30 μm along the crystallographic x direction. For single-pass OPG, the mixing waves travel from surfaces 1 to 4, and, for double-pass OPG, the mixing waves travel a round trip in the crystal between surfaces 1 and 2 through total

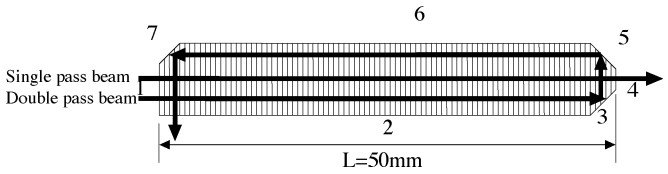

Fig. 5. Cutting configuration of the double-pass PPLN crystal, wherein all of the crystal surfaces, except surface 6, are optically polished. For single-pass OPG, the mixing waves travel from surfaces 1 to 4 and for double-pass OPG the mixing waves travel a round trip in the crystal between surfaces 1 and 2 through TIRs from surfaces 3, 5, and 7.

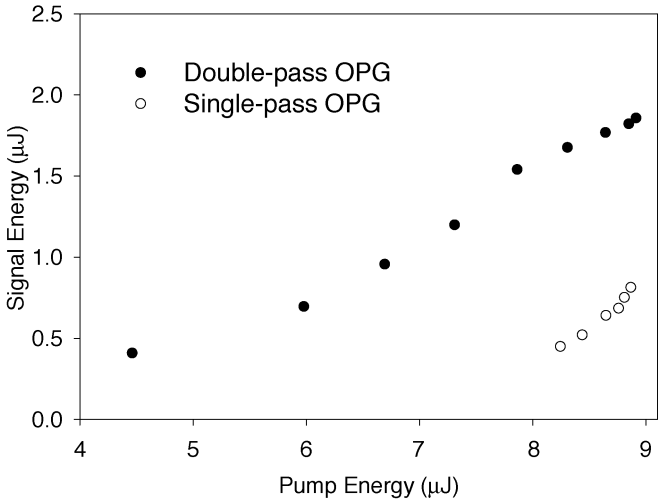

Fig. 6. Signal output energy versus the pump energy of the single-pass and double-pass OPGs phase-matched at 135 °C. The signal output energy from the double-pass OPG is enhanced from the single-pass OPG by more than a factor of 2.

internal reflections at surfaces 3, 5, and 7. For additional passes, one can cut an additional 45° reflection edge between surfaces 1 and 2. The polished total-internal-reflection (TIR) edges contribute almost no loss to the nonlinear frequency conversion process. The increased PPLN thickness, from 0.5 to 1 mm, is to avoid beam clipping at the crystal surfaces in the long gain path (~100 mm). The pump laser in this experiment was again a 1064-nm Nd:YAG microchip laser passively Q-switched by a Cr:YAG saturable absorber, producing 9-μJ pulse energy and 730-ps pulse width at a 6.5-kHz repetition rate. We focused the laser beam to a 60-μm-radius ($1/e^2$-intensity) waist (inside the PPLN crystal) near surface 4. Fig. 6 shows the measured signal output energy versus the pump energy of the single- and double-pass OPGs phase-matched at 135 °C. Because of the typical poorer poling quality of 1-mm-thick congruent PPLN crystals, the signal conversion efficiency is smaller than that produced from previous experiments using a 0.5-mm-thick PPLN crystal. Nonetheless, the signal output energy from the double-pass OPG is enhanced over the single-pass one by more than a factor of 2.

It is interesting to compare the temporal and spectral characteristics of the single-pass and double-pass OPGs. Fig. 7 shows the signal pulse widths of the single-pass (dashed line) and double-pass (continuous line) OPGs. The pulse width of the double-pass OPG (700 ps) is close to the pump pulse width and that of the single-pass OPG (227 ps) is much shorter than the pump one. The inset in the figure shows the depleted pump

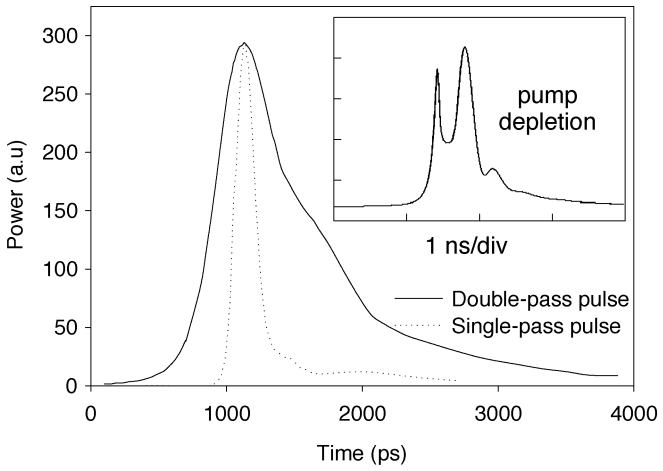

Fig. 7. Signal pulse widths of the single-pass and double-pass OPGs, wherein the double-pass one (continuous line) has a 700-ps FWHM pulsewidth and the single-pass one (dashed line) has a 227-ps FWHM pulsewidth. The inset in the figure shows the depleted pump pulse at the output of the double-pass OPG.

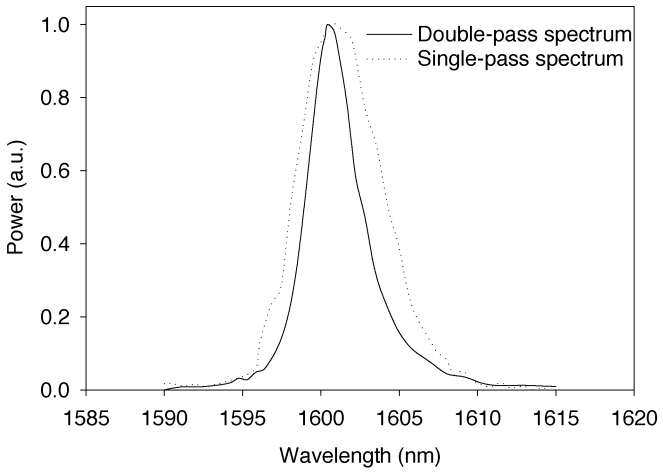

Fig. 8. Output signal spectra of the single-pass and double-pass OPGs. The single-pass OPG spectral width (dashed line) is 6 nm, whereas the double-pass one (continuous line) is reduced to 3.8 nm due to additional phase conditions at the TIR surfaces.

pulse of the double-pass OPG. Two obvious dips were observed in the depleted pulse. Due to the high pump intensity, the dip near the center of the pump pulse resulted from pump depletion when providing gain to the phase-matched components in the forward and backward passes. Since the pulse center was primarily depleted in the forward path, the pump intensity at the trailing edge in the asymmetrically pump-depleted pulse was relatively high in the backward path and was further pump depleted to generate additional OPG signal pulse. Therefore, the broadened signal pulse width for the double-pass OPG was caused by depleting two portions of the pump pulse during the two crystal transits.

Fig. 8 illustrates the output signal spectra of the single-pass and double-pass OPGs, wherein the double-pass OPG spectrum (continuous line) has a 3.8-nm spectral width and the single-pass one (dashed line) has a 6-nm spectral width. Physically, the spectral narrowing in the double-pass OPG is due to the additional phase conditions at the TIR boundaries. As shown by Brosnan and Byer [24], the spectral narrowing factor of a

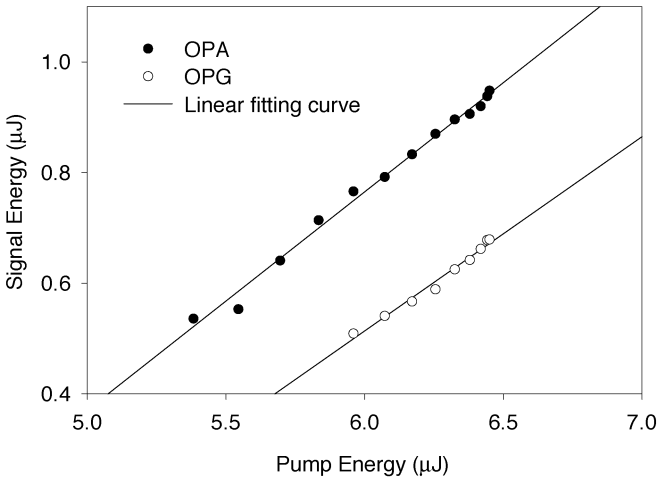

Fig. 9. OPA and OPG signal energy versus pump energy. The solid dots show OPA results and the open dots show OPG results. The power of the seeding diode laser was 0.6 mW. The slope efficiencies for the OPG and the OPA are 35.7% and 40.3%, respectively.

pulsed OPO is proportional to the square root of the number of the signal round trips in the OPO cavity. In our double-pass OPG experiment, all of the mixing waves propagated together and the OPG also had gain in the backward direction. Therefore, the theoretical spectral narrowing factor is approximately $\sqrt{2}$ for our double-pass OPG. From Fig. 8, the measured spectral narrowing factor of 1.58 is reasonably close to the theoretical value. This multipass OPG scheme is particularly useful for a modest pump power in a nonlinear optical material of a limited size.

D. Optical Parametric Amplification With Transform-Limited Output Linewidth

In order to show the potential of narrow-linewidth and diffraction-limited OPG outputs, Powers *et al.* presented some preliminary results of optical parametric amplification (OPA) in PPLN seeded by a diode laser [25]. Since DFB diode lasers emitting near the 1.55-μm telecommunication wavelengths are widely available, we show in the following a transform-limited, homogeneous-gain-broadened PPLN optical parametric amplifier seeded by a DFB diode laser and pumped by a transformed-limited microchip laser. In this experiment, the pump laser was a single-longitudinal-mode PQS Nd:YAG microchip laser operating at a 3.83-kHz rate with 530-ps FWHM pulse width. The DFB seeding diode laser produced 1.9-mW CW power at 1549.6-nm wavelength with a 35-MHz linewidth. The pump laser beam was focused to a 70-μm waist radius at the center of the PPLN crystal. The seeding power measured at the input end of the PPLN crystal was 0.6 mW. The PPLN crystal used in this experiment was 4 cm in length, 0.5 mm in thickness, and 30 μm in domain period. Both end faces of the PPLN crystal were optically polished and uncoated. The phase-matching temperature for the 1064-nm pumped OPA at the 1549.6-nm signal wavelength was 39.6 °C. Fig. 9 shows the internal signal energy versus internal pump energy of the unseeded OPG and the seeded OPA. For this measurement, the waist radius of the DFB diode laser at the center of the PPLN crystal was also about 70 μm. In the OPG experiment, the maximum signal conversion efficiency was 10.5% with 35.7% slope efficiency. In the

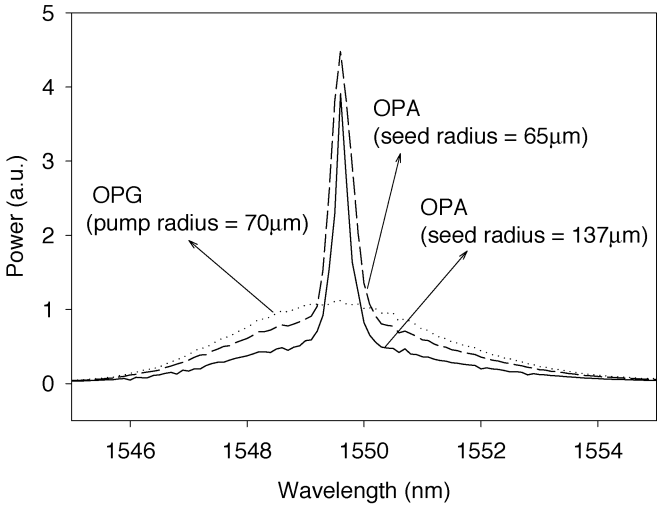

Fig. 10. Signal spectra of the seeded OPA and unseeded OPG. For a seed-laser beam size completely covering the pump beam size, homogeneous gain broadening in the optical parametric process can be seen from the plot as the two wings of the OPA spectra are lowered from the OPG spectrum.

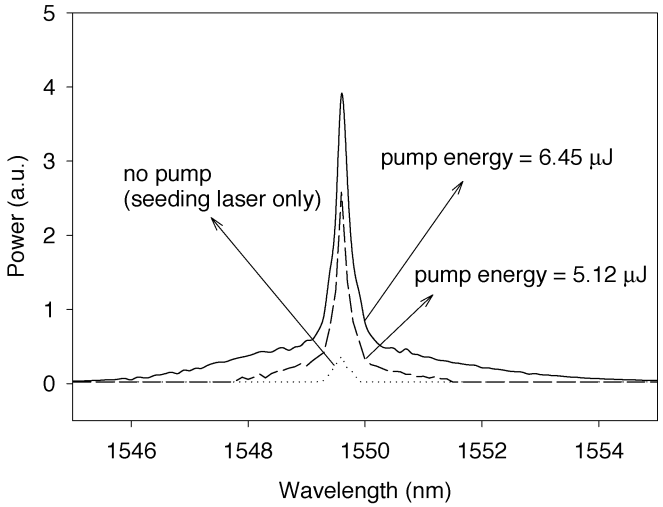

Fig. 11. OPA spectra for different pump energies for 137-μm seed-laser radius. Although the seed-laser beam completely covered the pump laser beam, the OPG background grew slightly as the pump power was increased.

seeded OPA experiment, the maximum conversion efficiency was 14.7% with 40.3% slope efficiency. Intuitively, one might expect that the energy output of the many-photon-seeded OPA would be much larger than that of the one-noise-photon-seeded OPG. In the experiment, the slight difference in the OPG and OPA outputs is attributable to the gain saturation from pump depletion. Despite the 530-ps pump pulse width, the generated OPA signal pulse width was only about 200 ps.

To understand the gain competition between OPA and OPG, initially we used a 1/2-m, 0.3-nm-resolution grating monochromator to characterize the signal spectrum. Fig. 10 shows the signal spectra of the seeded OPA and unseeded OPG. Homogeneous gain broadening in the optical parametric process can be seen from the plot as the two wings of the OPA spectra are lowered from the OPG spectrum. For this measurement, we intentionally varied the seed-laser waist radius with respect to the 70-μm pump waist radius. When the seed-laser radius was set to 65 μm, the OPA output spectrum contained some OPG energy due to the larger pump beam size. As soon as we expanded the seed-laser radius to 137-μm, the two OPG wings surrounding the OPA line center were noticeably reduced.

Fig. 11 shows the OPA spectra for different pump energies with the 137-μm seed-laser radius. Although the seed-laser beam completely covered the pump laser beam, the OPG background grew slightly as the pump power was increased. We suspected that, despite the spatial overlap between the seeding laser and the pump laser, the difference in the angular spectra between the two lasers could be the cause of the OPG background. The angular components of the pump laser that were not aligned with those of the seeding laser could grow independently when the pump intensity is strong enough for OPG. Nonetheless, with modest pump power and reasonable alignment, optical parametric amplification exhibited homogenous gain broadening in the PPLN optical parametric amplifier.

Fig. 12 shows the OPA signal spectrum measured from a scanning Fabry–Perot spectrometer under a 6.5-μJ pump energy. The scanning Fabry–Perot spectrometer has a free spectral range of 150 GHz and finesse of 1000. The inset of the figure

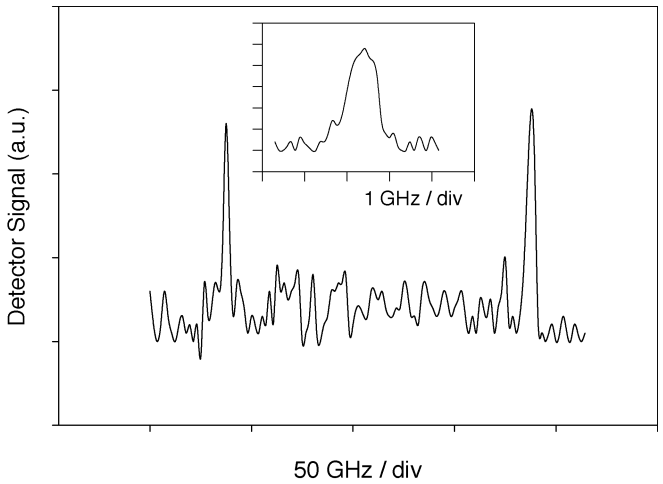

Fig. 12. OPA signal spectrum measured by a scanning Fabry–Perot spectrometer for 6.45 μJ pump energy. The separation between the two signal peaks is the 150-GHz free spectral range of the Fabry–Perot spectrometer. The noisy spectral floor resulted from the OPG background. The inset of the figure shows a fine scanned OPA signal spectrum, indicating a $\sim$1-GHz linewidth for the 200-ps signal pulse.

shows a fine scanned OPA signal spectrum, indicating a transform-limited 1-GHz linewidth for the 200-ps signal pulse. The noisy spectral floor resulted from the OPG background. Due to assorted telecommunication laser diodes near 1.5-μm wavelengths, this demonstration of narrow-line OPA can be extended to produce useful mid-infrared narrow-line radiations near 3-μm wavelengths.

III. Optical Parametric Oscillation

Optical parametric oscillators using PPLN as the nonlinear gain medium have been reported in a number of papers in the past few years [7], [17], [26]. In particular, infrared PPLN optical parametric oscillators have proven to be useful laser sources for various applications. Typical optical parametric oscillators involving external-cavity mirrors often require delicate alignment skills and cavity loss control. In this section, we

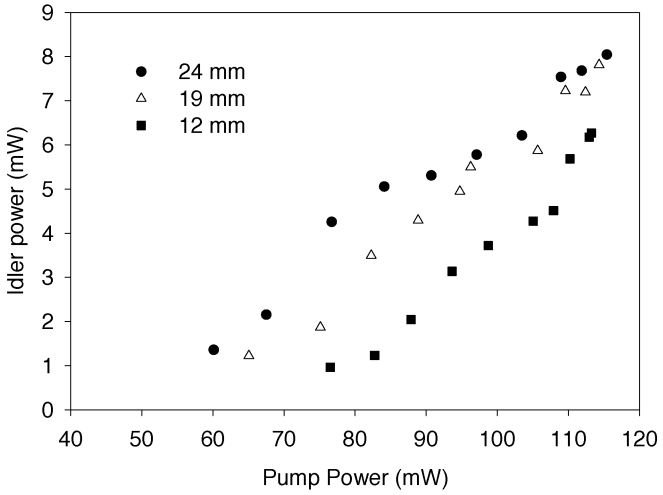

Fig. 13. Total idler power versus pump power for each monolithic PPLN optical parametric oscillator. When the average pump power was 115.4 mW, about 2.2 times above threshold, the 24-mm PPLN OPO produced 8.0-mW average power at the 3393-nm idler wavelength and, according to the Manley-Rowe relation, 17.4-mW power at the 1550-nm signal wavelength.

present two types of optical parametric oscillators in monolithic PPLN crystals.

Our first design of a monolithic PPLN optical parametric oscillator employs high-reflecting mirrors directly coated to the end faces of a polished PPLN crystal. To demonstrate this intrinsic-cavity optical parametric oscillator, we fabricated three pieces of PPLN crystals with 0.5-mm thickness and 29.6-μm domain period. The lengths of the three PPLN crystals were 12, 19, and 24 mm. Our interferometric fabrication technique guaranteed the parallelism of the two crystal end faces within 0.1°. The optically polished end faces were then directly coated with dielectric mirrors with reflectance higher than 99.5% between the 1520–1580-nm spectral range. The pumping source for the intrinsic-cavity PPLN optical parametric oscillator was again a PQS Nd:YAG microchip laser, producing 4.2-ns, 25-μJ laser pulses at a 7-kHz repetition rate. The peak power of the pump laser was about 6 kW that is not high enough for performing OPG in the three PPLN crystals. To establish oscillation, the 4.2-ns pulse width of this pump laser was longer than that used for our pervious OPG/OPA experiments.

While observing the OPO output power, we focused the pump laser beam to the center of each PPLN crystal and found that the optimal waist radii for the 12-, 19-, and 24-mm PPLN crystals were 53, 100, and 120 μm, respectively. The longer the crystal length, the larger the optimal pump waist radius and the less the diffraction loss. At about 22% power conversion efficiency in the 24-mm PPLN crystal, the signal spectral width centered at 1550 nm was measured to be 1 nm by using a 0.3-nm-resolution grating monochromator. The large spectral width was due to a limited number of roundtrip amplifications to the signal wave in such a planar-mirror resonator. Although the 4.2-ns pump pulse width was equal to 12 round trips in the 24-mm PPLN crystal, the effective number of round trips was greatly reduced due to diffraction in the planar-mirror resonator. For such a singly resonant optical parametric oscillator (SRO), the signal power can emit from both PPLN end faces, whereas the idler power primarily emits in the forward direction and a small but predictable amount in the backward direction due to reflection at the front face. To estimate the overall optical efficiency, we measured the idler power after a 2-mm-thick germanium filter in the forward direction and deduced the total signal power from the Manley–Rowe relation. We show in Fig. 13 the total idler output power versus pump power for each monolithic PPLN optical parametric oscillator. When the average pump power was 115.4 mW, about 2.2 times above threshold, the 24-mm PPLN OPO produced 8.0-mW average power at the 3393-nm idler wavelength and, according to the Manley–Rowe relation, 17.4-mW power at the 1550-nm signal wavelength. The overall optical power conversion efficiency exceeded 22%. The measured pulse width of the 1550-nm signal was approximately the same as the 4-ns pump pulse width, indicating that oscillation indeed was established in the planar-mirror resonator. From Fig. 13, for pump power less than $\sim$1.5 times above the threshold, the slope efficiency was close to the ratio of the idler photon energy to the pump photon energy or 32%. Due to pump depletion, the slope efficiency gradually decreased when the pump power was raised higher. These intrinsic-cavity optical parametric oscillators in monolithic PPLN crystals are relatively simple, compact, and efficient.

The second design of a monolithic PPLN optical parametric oscillator is what we called the DFB optical parametric oscillator. In such a device, a Bragg grating is built into a nonlinear optical material to establish single-longitudinal-mode parametric oscillation. In theory, a DFB optical parametric oscillator has the advantage of both mode selectivity and wavelength selectivity [27]. A DFB optical parametric oscillator also has the merit of laser oscillation in a nonlinear optical material longer than a pump pulse width. Previously, we have demonstrated optical parametric oscillation in PPLN crystals with built-in photorefractive DFB gratings [28]. The demonstration clearly showed parametric oscillation from monolithic PPLN crystals in both the visible and infrared spectra.

IV. Discussion and Conclusion

Optical parametric generators, amplifiers, and oscillators built upon monolithic PPLN crystals have the advantages of simplicity, compactness, high efficiency, and wide wavelength tunability. Passively Q-switched Nd:YAG lasers, producing modest peak power and subnanosecond pulse width with single longitudinal mode, are particularly suited for pumping those optical parametric devices.

For OPG, we derived and verified the spectral-width ratio between the high-gain and low-gain regimes. We also developed a theoretical model for the OPG signal in the pump-depleted high-gain regime. Both theories successfully explained the temporal and spectral characteristics of a series of single-pass and double-pass OPG experiments in monolithic PPLN crystals. In particular, a monolithic multipass PPLN crystal is a simple and efficient design for OPG with a modest pump power and a limited crystal size.

For optical parametric amplification, we demonstrated a transform-limited signal pulse from a diode-laser seeded and PQS-laser pumped PPLN optical parametric amplifier. For the first time, the homogeneous-gain-broadening phenomenon in OPA was observed. With a pump intensity sufficiently strong for optical parametric generation, spatial and angular

alignments for an optical parametric amplifier become critical for maintaining the homogeneous parametric linewidth.

For optical parametric oscillation, efficient intrinsic-cavity optical parametric oscillators were built and characterized in monolithic PPLN crystals. Pumped by a kW-level PQS Nd:YAG microchip laser, the overall optical conversion efficiency exceeded 22% in a 2.4-cm PPLN crystal. A DFB optical parametric oscillator holds great promises in both wavelength selectivity and mode selectivity for a coherent light source. DFB optical parametric oscillation in monolithic PPLN crystals was demonstrated in the visible and infrared spectra by using a pump pulse width shorter than the round-trip material length [28].

Recent advances in nonlinear optical materials have benefited QPM laser devices. Those improved materials, including impurity-doped congruent and stoichiometric lithium niobate [29] or lithium tantalite [30], give better efficiency, sustain higher laser intensity, provide a larger pump aperture, or reduce photorefractive damage and green-induced infrared absorption [31]. However, the temporal/spectral characteristics and the novel schemes of the monolithic optical parametric devices presented in this paper remain useful and valuable for developing efficient, high-quality, and compact laser devices.

ACKNOWLEDGMENT

The authors thank T.-C. Lin for help in fabricating several PPLN crystals.

REFERENCES

[1] S. E. Harris, "Tunable optical parametric oscillators," *Proc. IEEE*, vol. 58, pp. 2096–2113, Dec. 1969.

[2] R. G. Smith, "Optical parametric oscillators," in *Lasers*, A. K. Levine and A. J. DeMaria, Eds. New York: Dekker, 1976, pp. 189–307.

[3] R. A. Baumgartner and R. L. Byer, "Optical parametric amplification," *IEEE J. Quantum Electron.*, vol. QE-15, pp. 432–444, June 1979.

[4] J. A. Armstrong, N. Bloemergen, J. Ducuing, and P. S. Pershan, "Interactions between light waves in a nonlinear dielectric," *Phys. Rev.*, vol. 127, no. 6, pp. 1918–1939, Sept. 1962.

[5] M. Yamada, N. Nada, M. Saitoh, and K. Watanabe, "First-order quasiphase matched $LiNbO_3$ waveguide periodically poled by applying an external field for efficient blue second-harmonic generation," *Appl. Phys. Lett.*, vol. 62, no. 5, pp. 435–436, Feb. 1993.

[6] J. Webjörn, V. Prunery, P. S. J.P. St. J. Russel, J. R. M. Barr, and D. C. Hanna, "Quasiphase-matched blue light generation in bulk lithium niobate, electrically poled via periodic liquid electrodes," *Electron. Lett.*, vol. 30, no. 11, pp. 894–895, May 1994.

[7] L. E. Myers, G. D. Miller, R. C. Eckardt, M. M. Fejer, and R. L. Byer, "Quasiphase-matched 1.064-μm-pumped optical parametric oscillator in bulk periodically poled $LiNbO_3$," *Opt. Lett.*, vol. 20, no. 1, pp. 52–54, Jan. 1995.

[8] M. Taya, M. C. Bashaw, and M. M. Fejer, "Photorefractive effects in periodically poled ferroelectrics," *Opt. Lett.*, vol. 21, no. 12, pp. 857–859, June 1996.

[9] R. G. Batchko, G. D. Miller, and A. Alexandrovski *et al.*, "Limitations of high-power visible wavelength periodically poled lithium niobate devices due to green-induced infrared absorption and thermal lensing," in *Proc. Conf. on Lasers and Eletro-Optics*, vol. 6, Tech. Digest Series, Washington, DC, 1998, pp. 75–76.

[10] L. Huang, D. Huil, D. J. Bamford, S. J. Field, I. Mnushkina, L. E. Myers, and J. V. Kayser, "Periodic poling of magnesium-oxide-doped stoichiometric lithium niobate grown by the top-seeded solution method," *Appl. Phys. B*, vol. 72, no. 3, pp. 301–306, Feb. 2001.

[11] K. P. Petrov, S. Waltham, E. J. Dlugokencky, M. Arbore, M. M. Fejer, F. K. Tittel, and L. Hollberg, "Precise measurement of methane in air using diode-pumped 3.4-μm difference-frequency generation in PPLN," *Appl. Phys. B*, vol. 64, no. 5, pp. 567–572, May 1997.

[12] D. G. Lancaster, R. Weidner, D. Richter, F. K. Tittel, and J. Limpert, "Compact CH_4 sensor based on difference frequency mixing of diode lasers in quasiphasematched LiNbO3," *Opt. Commun.*, vol. 175, no. 461–468, Mar. 2000.

[13] T. Töpfer, K. P. Petrov, Y. Mine, D. Jundt, R. F. Curl, and F. K. Tittel, "Room-temperature mid-infrared laser sensor for trace gas detection," *Appl. Opt.*, vol. 36, no. 30, pp. 8042–8049, Oct. 1997.

[14] J. R. Bettis, R. A. House, and A. H. Guenther, *Laser Induced Damage in Optical Materials: 1976*, A. J. Glass and A. H. Guenther, Eds. Washington, DC: Nat. Bureau of Standards, 1977, p. 338.

[15] R. L. Byer, "Optical parametric oscillators," in *Treatise in Quantum Electronics*, H. Rabin and C. L. Tang, Eds. New York: Academic, 1973, pp. 587–702.

[16] J. J. Zayhowski, "Periodically poled lithium niobate optical parametric amplifiers pumped by high-power passively Q-switched microchip lasers," *Opt. Lett.*, vol. 22, no. 3, pp. 169–191, Feb. 1997.

[17] D. H. Jundt, "Temperature-dependent Sellmeier equation for index of refraction, n_e, in congruent lithium niobate," *Opt. Lett.*, vol. 22, no. 20, pp. 1553–1555, Oct. 1997.

[18] L. Lefort, K. Puech, G. W. Ross, Y. P. Svirko, and D. C. Hanna, "Optical parametric oscillation out to 6.3 μm in periodically poled lithium niobate under strong idler absorption," *Appl. Phy. Lett.*, vol. 73, no. 12, pp. 1610–1612, Sept. 1998.

[19] Y. C. Huang, A. C. Chiang, Y. Y. Lin, and Y. W. Fang, "Optical parametric generation covering the sodium D1, D2 lines from a 532-nm pumped PPLN with ionic-nonlinearity enhanced parametric gain," *IEEE J. Quantum Electron.*, vol. 38, pp. 1614–1619, Dec. 2002.

[20] A. C. Chiang, Y. C. Huang, Y. W. Fang, and Y. H. Chen, "A compact, 220-picosecond visible laser employing single-pass, cascaded frequency conversion in a monolithic periodically-poled lithium niobate," *Opt. Lett.*, vol. 26, no. 2, pp. 66–68, Jan. 2001.

[21] G. Imeshev, M. Proctor, and M. M. Fejer, "Phase correction in double-pass quasiphase-matched second-harmonic generation with a wedged crystal," *Opt. Lett.*, vol. 23, no. 3, pp. 165–167, Feb. 1998.

[22] Y. C. Huang, K. W. Chang, A. C. Chiang, T. C. Lin, B. C. Wong, and Y. H. Chen, "A high-efficiency nonlinear frequency converter with a built-in amplitude modulator," *J. Lightwave Technol.*, vol. 20, pp. 1165–1172, July 2002.

[23] T. H. Jeys, "Multipass optical parametric amplifier," *Opt. Lett.*, vol. 21, no. 16, pp. 1229–1231, Aug. 1996.

[24] S. J. Brosnan and R. L. Byer, "Optical parametric oscillator threshold and linewidth studies," *IEEE J. Quantum Electron.*, vol. QE-15, pp. 415–431, June 1979.

[25] P. E. Powers, P. K. Bojja, E. M. Vershure, and K. L. Schepler, "Narrowband mid-infrared generation in elliptically pumped periodically poled lithium niobate," in *Proc. Conf. Lasers and Electro-Optics, Tech. Digest CD-ROM*, Baltimore, MD, June 2003, paper CThG7.

[26] R. G. Batchko, D. R. Weise, T. Plettner, G. D. Miller, M. M. Fejer, and R. L. Byer, "Continuous-wave 532-nm-pumped singly resonant optical parametric oscillator based on periodically poled lithium niobate," *Opt. Lett.*, vol. 23, no. 3, pp. 168–170, Feb. 1998.

[27] Y. C. Huang and Y. Y. Lin, "Coupled-wave theory of distributed-feedback optical parametric amplifiers and oscillators," *J. Opt. Soc. Amer. B*, vol. 21, no. 4, pp. 1–13, Apr. 2004.

[28] A. C. Chiang, Y. Y. Lin, T. D. Wang, Y. C. Huang, and J. T. Shy, "Distributed-feedback optical parametric oscillation by use of a photorefractive grating in periodically poled lithium niobate," *Opt. Lett.*, vol. 27, no. 20, pp. 1815–1817, Oct. 2002.

[29] Y. Furukawa, J. Kitamura, S. Takekawa, K. Niwa, and H. Hatano, "Stoichiometric $Mg:LiNbO_3$ as an effective material for nonlinear optics," *Opt. Lett.*, vol. 23, no. 24, pp. 1892–1894, Dec. 1998.

[30] P. E. Bordui, R. G. Norwood, C. D. Bird, and J. T. Carella, "Stoichiometry issues in single-crystal lithium tantalite," *J. Appl. Phys.*, vol. 78, no. 7, pp. 4647–4650, Oct. 1995.

[31] Y. Furukawa, K. Kitamura, A. Alexandrovski, R. K. Route, M. M. Fejer, and G. Foulon, "Green-induced infrared absorption in MgO doped LiNbO3," *Appl. Phys. Lett.*, vol. 78, no. 14, pp. 1970–1972, Apr. 2001.

An-Chung Chiang revived the B.S. and M.S. degrees and the Ph.D. degree in electrical engineering from National Tsinghua University, Hsinchu, Taiwan, in 1997, 1999, and 2002, respectively.

Since 2003, he has been a Postdoctoral Associate with the Institute of Photonics Technologies, National Tsinghua University. His research interests include nonlinear optics, solid-state lasers, and laser-driven particle acceleration.

Dr. Chiang is a member of the Optical Society of America.

Tsong-Dong Wang received the B.S. degree in physics from Soochow University, Taipei, Taiwan, in 1999, and the M.S. degree in electrical engineering from National Tsinghua University, Hsinchu, Taiwan, in 2001. He is currently working toward the Ph.D. degree at National Chiaotung University, Hsinchu, Taiwan.

His research interests include nonlinear optics, solid-state lasers, and environmental sensing.

Yen-Yin Lin received the B.S. degree in atomic science and the M.S. degree in electrical engineering from National Tsinghua University, Hsinchu, Taiwan, in 2000 and 2002, respectively, where he is currently working toward the Ph.D. degree in electrical engineering.

His research interests include bio-photonics, nonlinear optics, and solid-state lasers.

Mr. Lin is a member of the Optical Society of America.

Chee-Wai Lau received the B.S. and M.S. degree in electrical engineering from National Tsinghua University, Hsinchu, Taiwan, in 2002. His thesis was on optical parametric generation and oscillation in monolithic PPLN crystals.

He is currently an R&D Engineer with AU Optronics Corporation, Hsinchu, Taiwan.

Yen-Hung Chen was born in Taichung, Taiwan, in 1968. He received the B.S. degree in nuclear engineering and the M.S. and Ph.D. degrees in nuclear science from National Tsing-Hua University (NTHU), Hsinchu, Taiwan, in 1991 and 1999, respectively.

He is currently a Postdoctoral Research Associate with the Department of Electrical Engineering, NTHU. His research interests are in the area of nonlinear optics and solid-state lasers.

Bi-Cheng Wong received the B.S. and M.S. degrees in physics from National Tsinghua University, Hsinchu, Taiwan, in 2002. His thesis was on the development of distributed feedback optical parametric oscillation in PPLN waveguides.

He is currently a System Engineer with ULi Electronics Inc., Taipei, Taiwan.

Yen-Chieh Huang (M'91) received the B.S. degree from National Sun Yat-Sen University, Kaohsiung, Taiwan, in 1987 and the M.S. and Ph.D. degrees from Stanford University, Stanford, CA, in 1991 and 1995, respectively, all in electrical engineering.

From 1995 to 1996, he was a Postdoctoral Research Affiliate with the Center for Nonlinear Optical Materials, Stanford University. During February 1997 and July 1999, he was an Assistant Professor with the Department of Atomic Science, National Tsinghua University, Hsinchu, Taiwan, where he is currently an Associate Professor with the Department of Electrical Engineering. His research interests include nonlinear optics, laser-driven electron acceleration, and optical environmental technologies.

Jow-Tsong Shy received the B.S. degree in physics from National Tsing Hua University, Hsinchu, Taiwan, in 1973, the M.S. degree in physics from the University of Illinois, Urbana-Champaign, in 1976, and the Ph.D. degree in optical sciences from the University of Arizona, Tucson, in 1982.

From 1982 to 1990, he was an Associate Professor with the Department of Physics, National Tsing Hua University, where he has been a Professor since 1990. His research interests include laser spectroscopy and laser frequency stabilization.

Yu-Pin Lan was born in I-Lan, Taiwan, R.O.C., in 1971. She received the B.S. degree in electronics engineering from Chung Yuan Christian University, Chung Li, Taiwan, in 1993 and the M.S. and Ph.D. degrees from National Chiao Tung University, Hsinchu, Taiwan, in 1996 and 2003, respectively.

Since 2003, she has been a Postdoctoral Associate with the Department of Electrophysics, National Chiao Tung University. Her main researches include laser technology and laser physics.

Yung-Fu Chen was born in Lukang, Taiwan, in 1968. He received the B.S. degree in electronics engineering and the Ph.D. degree from National Chiao Tung University, Hsinchu, Taiwan, in 1990 and 1994, respectively.

In 1994, he joined the Precision Instrument Development Center, National Science Council, Hsinchu, Taiwan where his research mainly concerns the development of diode-pumped solid-state lasers as well as quantitative analysis in surface electron spectroscopy. In 1999, he became an Associate Professor with the Department of Electrophysics, National Chiao Tung University, where he has been a Professor with the same department since 2002.

Pei-Hsi Tsao received the B.S., M.S., and Ph.D degrees in physics from National Taiwan University, Taipei, Taiwan, R.O.C., in 1967, 1969, and 1979, respectively.

He is currently a Professor with the Department of Physics, National Taiwan University. His research interests include nonlinear optics, spectroscopy, laser physics, laser safety, environmental application of photonics, biomedical application of photonics, and physics education.